Electronic Supplementary Information

Wide Bandgap Donor Polymers based on Dicyanodivinyl indacenodithiophene unit for Non-Fullerene Polymer Solar Cells

Baitian He*[a], Yulin Chen[a], Jinglong Chen[b], Songxi Chen[a], Manjun Xiao*[b], Guiting Chen*[a], Chuanbo Dai[a]

[a]School of Chemistry and Environment, Jiaying University, Guangdong Engineering Technology Developing Center of High- Performance CCL, Meizhou 514015, P. R. China

[b]College of Chemistry, Key Lab of Environment-Friendly Chemistry and Application (Ministry of Education), Xiangtan University, Xiangtan 411105, P. R. China

E-mail: baitian-he@foxmail.com

E-mail: xmj0704@163.com

E-mail: 576146400@qq.com

Experimental Section

***Materials*:** All solvents and reagents were purchased from commercial sources and used without further purification unless stated otherwise. All reactions were carried out under the nitrogen atmosphere. Tetrahydrofuran (THF) was distilled over sodium/benzophenone before use to ensure an anhydrous state. Monomer (M2), anhydrous N, N-Dimethylformamide (DMF), chlorobenzene (CB) and 1-chloronaphthalene were purchased from Sigma-Aldrich and used as received. Monomer (M4) and monomer (M5) were purchased from Derthon OPV Co Ltd. Monomer (M1) was prepared according to the previously reported literature.[1]

Measurements: Molecular weights of the copolymers were determined using an Agilent Technologies PL-GPC 220 high-temperature chromatograph in 150 °C and 1,2, 4-trichlorobenzene using a calibration curve of polystyrene standards. UV-vis absorption spectra were recorded on a SHIMADZU UV-3600 spectrophotometer. Cyclic voltammetry (CV) was carried out on a CHI660A electrochemical workstation with platinum electrodes at a scan rate of 50 mV s^{-1} against saturated calomel electrode (SCE) and a platinum wire as reference electrode with nitrogen-saturated solution of 0.1 M tetrabutylammonium hexafluorophosphate in acetonitrile. Potentials were referenced to the 2 ferrocenium/ferrocene couple by using ferrocene as an internal standard. The deposition of a copolymer on the electrode was done by the evaporation of a chlorobenzene solution. Tapping-mode atomic force microscopy (AFM) images were obtained using a NanoScope NS3A system (Digital Instrument). Transmission electron microscopy (TEM) images were obtained using a JEM-2100F instrument.

DFT Calculations. The geometry was optimized with Density Functional Theory (DFT) using B3LYP hybrid functional with basis set 6-31g*. Quantum-chemical calculation was performed with the Spartan 10 software. All alkyl chains were ignored in order to simplify the calculations.

Charge Carrier Mobility Measurements. The hole-only and electron-only devices

were measured with device structures of ITO/PEDOT:PSS/Copolymer:Y6/MoO_3/Al and ITO/ZnO/Copolymer:Y6/Ca/Al, respectively. The mobility was determined by fitting the dark current to the model of a single-carrier SCLC, which is described by the following equation:

$$J = \frac{9}{8}\varepsilon_0\varepsilon_r\mu_0\frac{V^2}{d^3}$$

where J is the current, μ_0 is the carrier mobility, ε_0 is the permittivity of free space, ε_r is the relative permittivity of the material, d is the thickness of the active layer, and V is the effective voltage. The effective voltage can be obtained by subtracting the built-in voltage (V_{bi}) and the voltage drop (V_s) from the substrate's series resistance from the applied voltage (V_{appl}), i.e., $V = V_{appl} - V_{bi} - V_s$. The carrier mobility can be calculated from the slope of the $J^{1/2}$–V curves.

***Fabrication of Polymer Solar Cells and Characterization*:** The indium tin oxide (ITO) glass substrates were cleaned sequentially under sonication for 30 min with acetone, detergent, deionized water and isopropyl alcohol and then dried at 80 °C in baking oven overnight, followed by a plasma treatment for 4 min. The pre-cleaned ITO substrate were coated with ZnO (filtered through a 0.45 μm PES filter) by spin-coating (3000 rpm. for 30 s, thickness of ~40 nm) and then baked at 150 °C for 15 min in air. Then, the substrates were transferred into a nitrogen (N_2) protected glovebox. The device configuration was ITO/ ZnO/active layer/MoO_3/Al, and the active layers were spin coated from chloroform solution containing Donor:Y6 (weight ratio 1:1.2) to obtain thicknesses of ~100 nm for PBDT or PBDT-S. Thermal annealing of the blend films was carried out by placing them onto a hot plate in a nitrogen atmosphere. The thin films were transferred into a vacuum evaporator connected to the glove box, and Al (90 nm) was deposited sequentially through a shadow mask under 10^{-7} Pa, with an active area of the cells of 0.04 cm^2.

The current–voltage (J–V) curves were measured on a computer-controlled Keithley 2400 sourcemeter under 1 sun, AM 1.5 G spectra from a class solar simulator (Taiwan,

Enlitech), and the light intensity was 100 mW cm^{-2} as calibrated by a China General Certification Center certified reference monocrystal silicon cell (Enlitech). Before the *J–V* test, a physical mask of an aperture with a precise area of 0.04 cm^2 was used to define the device area. The EQE data were recorded with a QE-R3011 test system from Enli technology company (Taiwan).

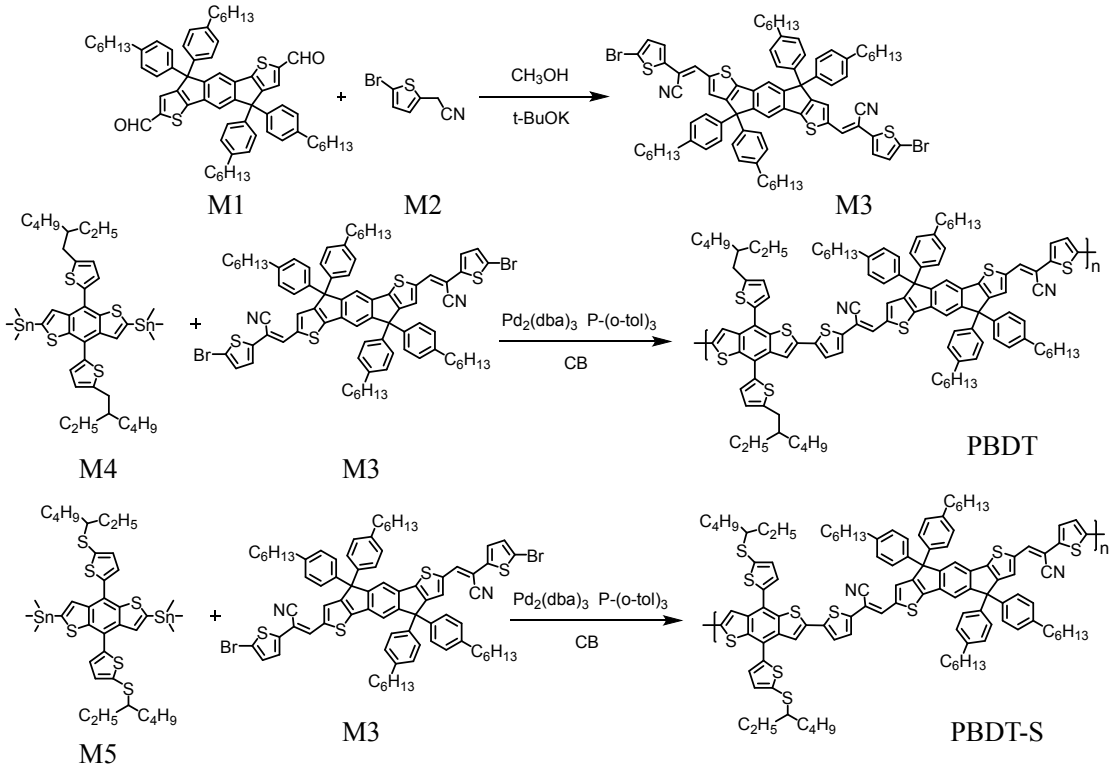

Scheme S1. Synthetic route to monomers and copolymers.

Synthesis of the monomers

(2E,2'E)-3,3'-(4,4,9,9-tetrakis(4-hexylphenyl)-4,9-dihydro-s-indaceno[1,2-b:5,6-b']dithiophene-2,7-diyl)bis(2-(5-bromothiophen-2-yl)acrylonitrile) (M3).[2] Monomer 1 (2.41 g, 2.5 mmol) and Monomer 2 (1.01 g, 5.0 mmol) were dissolved in methanol (25 mL). The mixture was added with a catalytic amount of potassium tert-butoxide solution in methanol with gentle stirring and allowed to react for 2 days at room temperature. The product was obtained as a precipitate, which was collected by filtration and washed with methanol. The crude product was purified by column chromatography on silica (4:1 PE and DCM) , then recrystallized from acetonitrile to

get the product as yellow solid (4.66 g, yield 70%). ^{1}H NMR (500 MHz, $CDCl_3$), δ (ppm): δ 7.52 (s, 2H), 7.38 (s, 2H), 7.30 (s, 2H), 7.14 (d, J = 8.3 Hz, 4H), 7.09 (d, J = 8.3 Hz, 4H), 7.03 (d, J = 3.9 Hz, 2H), 6.99 (d, J = 3.9 Hz, 2H), 2.62 – 2.52 (m, 8H), 1.64 – 1.52 (m, 8H), 1.39 – 1.21 (m, 24H), 0.88 (t, J = 6.9 Hz, 12H). ^{13}C NMR (125 MHz, $CDCl_3$), δ (ppm): 154.61, 150.50, 146.65, 144.40, 142.35, 141.77, 140.21, 139.73, 139.21, 131.44, 129.86, 128.74, 128.53, 127.84, 118.91, 118.35, 118.02, 113.74, 64.32, 35.73, 31.80, 31.27, 28.91, 22.70, 14.10. MS (ESI): calculated for $C_{78}H_{78}Br_2N_2S_4$ [M^+], 1331.54; found: 1331.03.

Synthesis of the copolymers

PBDT. To a mixture of monomer M3 (133.15mg, 0.1 mmol), monomer M4 (90.46 mg, 0.1 mmol) and 1.6 mL chlorobenzene were added to a 35 mL flask protected with N_2. The mixture was purged with N_2 for 15 min. Then catalyst $Pd_2(dba)_3$ (2.5 mg) and P(o-tol)$_3$ (5 mg) was quickly added under a stream of N_2, and the mixture was purged with argon for another 15 min. Subsequently, the reaction mixture was then sealed and heated at 160 °C for 2 days. After cooling to room temperature, the reaction mixture was poured into a mixture of methanol (100 mL), the solid was collected by filtration and loaded into an extraction thimble and washed successively with methanol, acetone, hexane, dichloromethane and chlorobenzene. The chlorobenzene solution was then concentrated by evaporation, precipitated into methanol. The solid was collected by filtration and dried in vacuo to get the copolymer as a black solid (156.5 mg, 88.8%). Mn= 37.6 kDa, Mw= 86.1 kDa, PDI= 2.29.

PBDT-S was synthesized according to the similar procedures for **PBDT** from corresponding monomers (154.25 mg, 85.0%). Mn= 36.8 kDa, Mw= 104.1 kDa, PDI= 2.83.

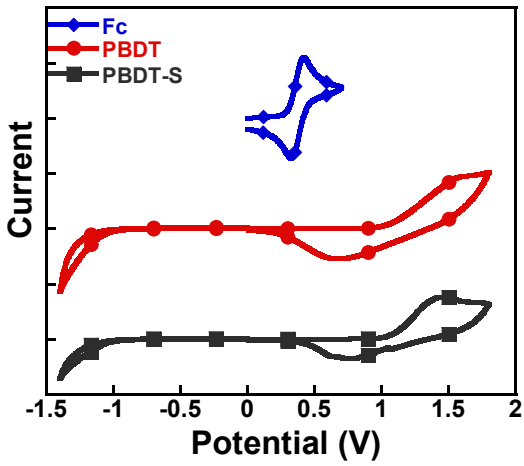

Fig. S1. CV curves of the donor copolymers.

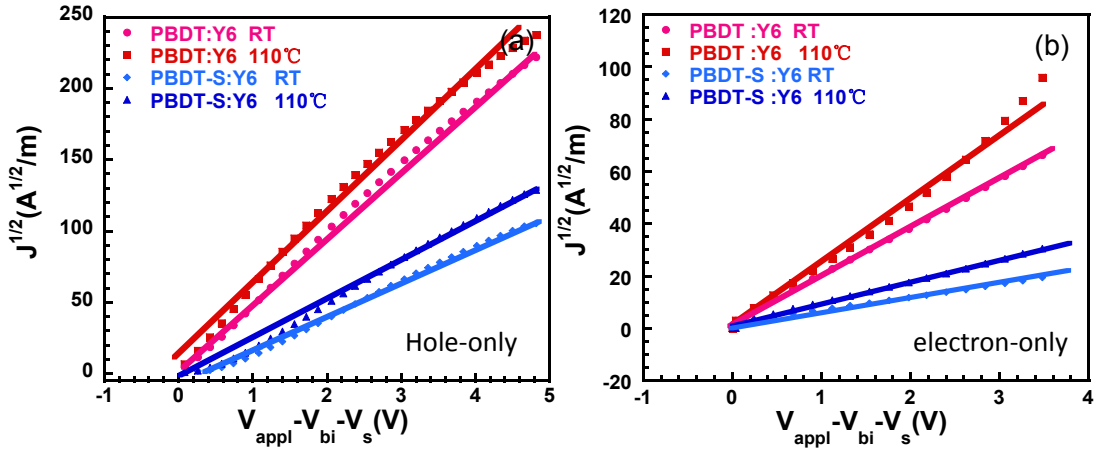

Fig. S2 $J^{1/2}$~(V_{appl}-V_{bi}-V_s) characteristics of hole-only and electron-only devices.

Table S1. Device performance of the NF-PSCs based on PBDT:Y6 with various thermal annealing temperature.

Blend films[a]	Thermal annealing	V_{oc} (V)	J_{sc} (mA/cm^2)	FF (%)	PCE (%)
PBDT:Y6	none	0.88	18.74	50.60	8.41
	90°C	0.88	21.40	50.81	9.55
	110°C	0.88	22.16	51.31	10.04
	130°C	0.87	20.68	49.97	9.03

[a]All of the blend films are processed by CF and Donor:Acceptor =1:1.2.

Table S2. Device performance of the NF-PSCs based on PBDT:Y6 with different D/A

ratios.

Blend films[a]	D/A (wt/wt)	V_{OC} (V)	J_{SC} (mA/cm^2)	FF (%)	PCE (%)
PBDT:Y6	1:0.8	0.88	19.09	50.51	8.49
	1:1.2	0.88	22.16	51.31	10.04
	1:1.6	0.88	21.13	51.56	9.61
	1:2	0.87	20.18	53.80	9.44

[a] All of the blend films are processed by CF and with thermal annealing at 110 °C.

Table S3. Device performance of the PSCs based on PBDT:Y6 with different additive ratio.

Blend films[a]	CN (v/v)	V_{OC} (V)	J_{SC} (mA/cm^2)	FF (%)	PCE (%)
PBDT:Y6	none	0.88	22.16	51.31	10.04
	0.5%	0.88	20.57	44.61	8.05

[a] All of the blend films are processed by Donor:Acceptor =1:1.2 and with thermal annealing at 110 °C.

Table S4. Device performance of the PSCs based on PBDT:Y6 with different speed.

Blend films[a]	Speed (rpm)	V_{OC} (V)	J_{SC} (mA/cm^2)	FF (%)	PCE (%)
PBDT:Y6	1600	0.82	12.68	48.90	5.08
	1800	0.84	13.69	56.74	6.51
	2000	0.84	13.96	57.33	6.73
	2200	0.84	12.88	56.28	6.09

[a] All of the blend films are processed by THF and Donor:Acceptor =1:1.2.

Table S5. Device performance of the PSCs based on PBDT:Y6 with different additive.

Blend films[a]	additive	V_{OC} (V)	J_{SC} (mA/cm^2)	FF (%)	PCE (%)
PBDT:Y6	1%DIO	0.82	17.36	58.85	8.41
	1%CN	0.81	9.89	49.40	3.95

[a] All of the blend films are processed by THF and Donor:Acceptor =1:1.2.

Table S6. Device performance of the PSCs based on PBDT:Y6 with different additive ratio.

Blend films[a]	ratio	V_{OC} (V)	J_{SC} (mA/cm^2)	FF (%)	PCE (%)
PBDT:Y6	w/o	0.84	13.96	57.33	6.73
	0.5%	0.83	14.42	58.59	7.04
	1%	0.82	17.36	58.85	8.41
	1.5%	0.82	17.24	58.91	8.35
	2%	0.82	16.92	59.40	8.21

[a] All of the blend films are processed by THF and Donor:Acceptor =1:1.2.

Table S7. Device performance of the PSCs based on PBDT:Y6 with different device area.

Blend films[a]	Device area	V_{OC} (V)	J_{SC} (mA/cm^2)	FF (%)	PCE (%)
PBDT:Y6	0.04 cm^2	0.88	22.16	51.31	10.04
	0.08 cm^2	0.88	17.19	47.15	7.16
	1 cm^2	0.89	17.41	42.72	6.93

Table S8. Relevant parameters obtained from J_{ph}–V_{eff} curves.

Blend films [a]	annealing	J_{sat} (mA cm^{-2})	G_{max} (m^{-3} s^{-1})	L (nm)
PBDT:Y6	w/o	21.49	1.34×10^{27}	100
PBDT:Y6	110 ℃	24.87	1.55×10^{27}	100
PBDT-S:Y6	w/o	18.17	1.14×10^{27}	100
PBDT-S:Y6	110 ℃	19.43	1.21×10^{27}	100

[a] Donor : Acceptor =1:1.2; all of the blend films are processed by CF. [b] At the condition of $V_{eff} = V_0 - V_{appl}$ ($V_{appl} = 0$, under short-circuit condition).

Table S9. Photovoltaic results of high performance PSCs devices based on Y6 as acceptor.

Active layers	Device structure	Processing	Size	PCE(%)	References
PM6:Y6	ITO/PEDOT:PSS/PM6:Y6/ PDINO/Al	spin-cast	5 mm^2	15.7	S3
S1:Y6	ITO/ PEDOT:PSS/active layer/Zracac/Al.	spin-coating	5.9 mm^2	16.4	S4
P2F-EHp: Y6	ITO/PEDOT:PSS/active layer/PFNDI-Br/Ag	spin-coating	4 mm^2	16.02	S5
D18:Y6	ITO/PEDOT:PSS/D18:Y6/ PDIN/Ag	spin-coating	4 mm^2	18.2	S6
PE2:Y6	ITO/ PEDOT: PSS/active layer/ Ca/ Al	spin-coating	0.04 cm^2	13.5	S7
PIDTT-DTffBTA:Y6	/ITO/PEDOT:PSS/active layer/Ca/Al	spin-coating	0.04 cm^2	11.0	S8
PBiTPD:Y6	ITO/PEDOT:PSS/Donor:Y6/ PFN-Br/Ag	spin-coating	0.04 cm^2	14.2	S9
PM7:Y6	ITO/PEDOT:PSS/active layers/PNDIT-F3N/Ag	spin-coating	5.9 mm^2	17.0	S10
P2:Y6	ITO/PEDOT:PSS/active layer/PDINO/Al	spin-coating	4 mm^2	15.1	S11
W1:Y6	ITO/PEDOT:PSS/W1:Y6/ PDIN/Ag	spin-coating	4 mm^2	16.2	S12
PTQ10:Y6	ITO/PEDOT:PSS/active layer/PDINO/Al	spin-coating	7.5 mm^2	16.5	S13
PBDT:Y6	ITO/ZnO/active layer/MoO_3/Al	spin-coating	0.04 cm^2	10.04	This work

S1 Y. Lin, J. Wang, Z. G. Zhang, H. Bai, Y. Li, D. Zhu and X. Zhan, *Adv. Mater.*, 2015, **27**, 1170–1174.

S2 B. He, Q. Yin, X. Yang, L. Liu, X.-F. Jiang, J. Zhang, F. Huang and Y. Cao, *J. Mater. Chem. C*, 2017, **5**, 8774–8781.

S3 J. Yuan, Y. Zhang, L. Zhou, G. Zhang, H. L.Yip, T. K. Lau, X. Lu, C. Zhu, H. Peng, P. A. Johnson, M. Leclerc, Y. Cao, J. Ulanski, Y. Li and Y. Zou, *Joule*, 2019, **3**, 1–12.

S4 H. Sun, T. Liu, J. Yu, T.-K. Lau, G. Zhang, Y. Zhang, M. Su, Y. Tang, R. Ma, B.

Liu, J. Liang, K. Feng, X. Lu, X. Guo, F. Gao and H. Yan, *Energy Environ. Sci*., 2019, **12**, 3328–3337.

S5 B. Fan, D. Zhang, M. Li, W. Zhong, Z. Zeng, L. Ying, F. Huang and Y. Cao, *Sci. China Chem*., 2019, **62**, 746-752.

S6 Q. Liu, Y. Jiang, K. Jin, J. Qin, J. Xu, W. Li, J. Xiong, J. Liu, Z. Xiao, K. Sun, S. Yang, X. Zhang and L. Ding, *Sci. Bull.*, 2020, **65**, 272–275.

S7 Y. Chen, Y. Geng, A. Tang, X. Wang, Y. Sun and E. Zhou, *Chem. Commun*., 2019, **55**, 6708—6710.

S8 F. Li, A. Tang, B. Zhang, and E. Zhou, *ACS Macro Lett*. 2019, **8**, 1599−1604.

S9 J. Zhao, Q. Li, S. Liu, Z. Cao, X. Jiao, Y.-P. Cai and F. Huang, *ACS Energy Lett*., 2020, **5**, 367–375.

S10 R. Ma, T. Liu, Z. Luo, Q. Guo, Y. Xiao, Y. Chen, X. Li, S. Luo, X. Lu, M. Zhang, Y. Li and H. Yan, *Sci. China Chem*., 2020, **63**, 325–330.

S11 W. Li, Q. Liu, K. Jin, M. Cheng, F. Hao, W.-Q. Wu, S. Liu, Z. Xiao, S. Yang, S. Shi and L. Ding, *Mater. Chem. Front*., 2020, **4**, 1454–1458.

S12 T. Wang, J. Qin, Z. Xiao, X. Meng, C. Zuo, B. Yang, H. Tan, J. Yang, S. Yang, K. Sun, S. Xie and L. Ding, *Sci. Bull*., 2020, **65**, 179–181.

S13 Y. Wu, Y. Zheng, H. Yang, C. Sun, Y. Dong, C. Cui, H. Yan and Y. Li, *Sci. China Chem*., 2020, **63**, 265–271.